Mechanics of Materials 105 (2017) 49–60

Contents lists available at ScienceDirect

Mechanics of Materials

journal homepage: www.elsevier.com/locate/mechmat

Micromechanics-based simulations of compressive and tensile testing on lime-based mortars

V. Nežerka*, J. Zeman, J. Němeček

Faculty of Civil Engineering, Czech Technical University in Prague, Thákurova 7, 166 29 Praha 6, Czech Republic

ARTICLE INFO

Article history:
Received 3 December 2015
Revised 11 November 2016
Available online 1 December 2016

Keywords:
Micromechanics
Stiffness
Strength
Fracture energy
Mori–Tanaka method
Mortar
Shrinkage cracking

ABSTRACT

The purpose of this paper is to propose a continuum micromechanics model for the simulation of uniaxial compressive and tensile tests on lime-based mortars, in order to predict their stiffness, compressive and tensile strengths, and tensile fracture energy. In tension, we adopt an incremental strain-controlled form of the Mori–Tanaka scheme with a damageable matrix phase, while a simple J_2 yield criterion is employed in compression. To reproduce the behavior of lime-based mortars correctly, the scheme must take into account shrinkage cracking among aggregates. This phenomenon is introduced into the model via penny-shaped cracks, whose density is estimated on the basis of particle size distribution combined with the results of finite element analyses of a single crack formation between two spherical inclusions. Our predictions show a good agreement with experimental data and explain the advantages of compliant crushed brick fragments, often encountered in ancient mortars, over stiff sand particles. The validated model provides a reliable tool for optimizing the composition of modern lime-based mortars with applications in conservation and restoration of architectural heritage.

1. Introduction

Lime-based mortars were widely used as masonry binder in ancient times (Moropoulou et al., 2000a; Maravelaki-Kalaitzaki et al., 2003). Nowadays, they are often required by the authorities for cultural heritage for repairs of old masonry because of their compatibility with the original materials (Sepulcre-Aguilar and Hernández-Olivares, 2010; Callebaut et al., 2001). The substitution of lime-based mortars with binders based on Portland cement turned out to be inappropriate, because of the damage to the original masonry due to high stiffness contrast and to the presence of solutable salts (Veniale et al., 2003). On the other hand, the calcitic matrix of pure lime mortars is relatively weak, more compliant (Arizzi and Cultrone, 2012; Lanas et al., 2004), and susceptible to shrinkage up to 13% (Nežerka et al., 2014a; Wilk et al., 2013).

To improve the durability and strength of ancient mortars, masons often used additives rich in silica (SiO_2) and alumina (Al_2O_3) (Arizzi and Cultrone, 2012; Velosa et al., 2009; Papayianni and Stefanidou, 2007) in the form of volcanic ash or crushed ceramic bricks, tiles or pottery (Moropoulou et al., 2005; Farci et al., 2005). In recent years, metakaolin has become a very popular alternative to these ancient additives, because of its high reactivity, e.g. Murat (1983); Adami and Vintzileou (2007); Velosa et al. (2009); Moropoulou et al. (2004). On the other hand, the crushed brick fragments are considered as a rather inert aggregate since the hydraulic reaction, if at all, can take place only at the interface between the fragments and the surrounding matrix. Moreover, the formation of hydraulic products requires the presence of moisture (Baronio and Binda, 1997), a significant amount of time (Moropoulou et al., 2002), and ceramic clay fired at appropriate temperatures (Bakolas et al., 2008). Beside using the matrix-enhancing additives, the mechanical properties of lime mortars can be also improved by optimizing the amount and composition of aggregates (Arizzi and Cultrone, 2012; Lanas et al., 2004; Stefanidou and Papayianni, 2005), mostly via a time-demanding trial-and-error procedure.

The goal of this paper is to render the design process more efficient by proposing a simple model for the prediction of basic properties of lime-based mortars in tension and compression. Our developments have been inspired by earlier studies dealing with micromechanics of cement pastes in compression (Pichler and Hellmich, 2011) and in tension (Vorel et al., 2012). The first study by Pichler and Hellmich (2011) exploited a two-level homogenization approach combining the self-consistent (Hill (1965); Budiansky (1965) ; Mori and Tanaka (1973); Benveniste (1987)) schemes and a J_2-based criterion to estimate the compressive strength. In their later work, Vorel et al. (2012) estimated the tensile strength and fracture energy by combining the incremental

* Corresponding author.
E-mail addresses: vaclav.nezerka@fsv.cvut.cz, vaclav.nezerka@gmail.com (V. Nežerka), zemanj@cml.fsv.cvut.cz (J. Zeman), jiri.nemecek@fsv.cvut.cz (J. Němeček).

http://dx.doi.org/10.1016/j.mechmat.2016.11.011
0167-6636/

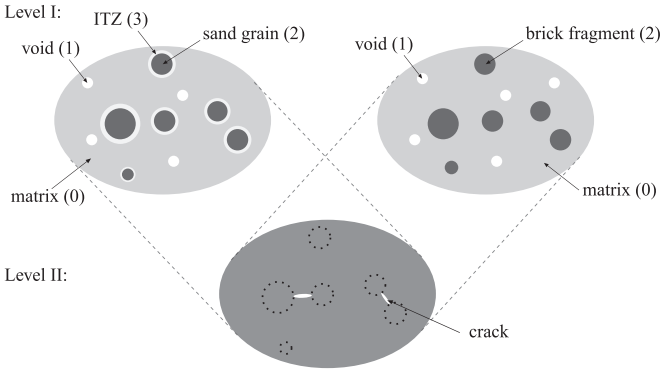

Fig. 1. Scheme of the micromechanical model of mortars with various aggregate-types; the numbers in parentheses refer to the indexes of individual phases.

form of the Mori–Tanaka method at a single-level with the crack band model (Bažant and Oh, 1983) to account for the distributed matrix cracking.

A related study into the pre-peak response of cementitious materials under uniaxial compression was conducted by Kuo et al. (2008). In their approach, the matrix phase was represented by the viscoelastic Burgers model and the overall behavior was obtained by a secant Mori–Tanaka scheme, while assuming a constant strain rate. This model was extended later by Pan and Weng (2010); 2012) to include, respectively, rate- and age-dependent effects in the Burgers model. However, the crucial feature missing from all the models is the effect of drying shrinkage-induced cracks that are intrinsic to the mechanical properties of lime-based mortars.

Shrinkage-induced cracking in cement-like materials has been addressed by both modeling and experimental studies. A detailed analytical investigation into shrinkage cracking around a single cylindrical aggregate was performed by Dela and Stang (2000) to estimate crack growth in high-shrinkage cement paste. The behavior of multi-aggregate systems was addressed numerically by Grassl et al. (2010) using a discrete lattice model; their findings were in agreement with the cracking patterns observed by Bisschop and van Mier (2002). Backscattered electron microscopy (BSE) confirmed that the lime-based mortars rich in sand suffer from an extensive matrix cracking (Stefanidou and Papayianni, 2005). Based on these studies and also on our independent experimental investigations (Nežerka et al., 2014a; 2015), we decided to represent the shrinkage cracks as penny-shaped polydisperse voids in our homgenization scheme.

Based on these considerations, the model proposed in Section 2 operates at two scales; see Fig. 1. At Level I, we account for the individual components of mortar, such as lime matrix, sand or brick particles, and distributed voids. At Level II, the shrinkage cracks are introduced into the homogenized material from Level I. Details of this procedure are provided in Section 2.1, with the goal to estimate initial elastic properties by the Mori–Tanaka procedure at Level I, Section 2.1.1, and the dilute approximation at Level II, Section 2.1.2. The density and size distribution of the penny-shaped shrinkage cracks are determined from a crack formation criterion, proposed in Section 2.1.3 on the basis of three-dimensional finite element analyses of shrinkage-induced cracking between two isolated inclusions. Two extensions of the elastic model are presented next. The strength under stress-controlled uniaxial compression is estimated in Section 2.2 on the basis of the J_2 stress invariant in the matrix phase. Under strain-controlled uniaxial tension, Section 2.3, we employ the incremental form of the Mori–Tanaka scheme coupled with an isotropic damage constitutive model to estimate the tensile strength and fracture energy. Note that our model does not account for viscoelastic effects at the matrix level, so its predictions are independent of age and loading rate.

Having introduced our model, in Section 3 we specify the input data for individual components, along with the experimental procedures used to acquire them, and the composition of the tested mortar samples. Section 4 is dedicated mostly to the model validation, concluded by the determination of the optimal mix composition. Finally, we summarize our results in Section 5 and outline our strategy to translate them to the structural scale.

In the following text, the condensed Mandel representation of symmetric tensorial quantities is employed; see e.g. Milton (2002). In particular, the scalar quantities are written in the italic font, e.g. a or A, and the boldface font, e.g. $\mathbf{a}$ or $\mathbf{A}$, is used for vectors or matrices representing second- or fourth-order tensors. $\mathbf{A}^{\mathrm{T}}$ and $(\mathbf{A})^{-1}$ denote the matrix transpose and the inverse matrix, respectively. Other symbols are introduced later, when needed.

2. Model

We consider an RVE occupying a domain Ω, composed of m phases indexed by r at Level I, and penny-shaped shrinkage-induced cracks reflected at Level II. The matrix is represented by $r = 0$ and indexes $r = 1, \ldots, m$ refer to heterogeneities of spherical shape or spherical shell in the case of interfacial transition zone (ITZ) around sand grains; see Fig. 1. The volume fraction of r-th phase, having the volume $|\Omega^{(r)}|$, is provided by $c^{(r)} = |\Omega^{(r)}|/|\Omega|$. Note that the representation of sand / crushed brick particles by spheres is less realistic then e.g. by ellipsoids (Pichler et al., 2009), but the effect of the introduced errors is minor relative to the accuracy of the input data, cf. Section 3. The modeling assumptions are summarized in Table 1.

2.1. Elasticity

2.1.1. Level I: homogenization of aggregates and voids

The elastic response of individual phases is described by the material stiffness matrix $\mathbf{L}^{(r)}$. Since all phases are considered as geometrically and materially isotropic, the matrix $\mathbf{L}^{(r)}$ can be decomposed using the orthogonal volumetric and deviatoric projections $\mathbf{I}_{\mathrm{V}}$ and $\mathbf{I}_{\mathrm{D}}$, e.g. Milton (2002, p. 23),

$$\mathbf{L}^{(r)} = 3K^{(r)}\mathbf{I}_{\mathrm{V}} + 2G^{(r)}\mathbf{I}_{\mathrm{D}}, \tag{1}$$

where $K^{(r)}$ and $G^{(r)}$ denote the bulk and shear moduli of the rth phase.

Under the dilute approximation, the mean strain in individual phases, $\boldsymbol{\varepsilon}^{(r)}$, is related to the macroscopic strain, $\boldsymbol{\varepsilon}$, via the dilute concentration factors:

$$\boldsymbol{\varepsilon}^{(r)} = \mathbf{A}_{\mathrm{dil}}^{(r)}\boldsymbol{\varepsilon}. \tag{2}$$

In the Mori–Tanaka scheme, the strain in individual phases can be found as $\boldsymbol{\varepsilon}^{(r)} = \mathbf{A}_{\mathrm{dil}}^{(r)}\boldsymbol{\varepsilon}^{(0)}$, where $\boldsymbol{\varepsilon}^{(0)}$ is the strain within the matrix found as

$$\boldsymbol{\varepsilon}^{(0)} = \mathbf{A}_{\mathrm{MT}}\boldsymbol{\varepsilon}, \tag{3}$$

where the strain concentration factor $\mathbf{A}_{\mathrm{MT}}$ is provided by

$$\mathbf{A}_{\mathrm{MT}} = \left(c^{(0)}\mathbf{I} + \sum_{r=1}^{m} c^{(r)}\mathbf{A}_{\mathrm{dil}}^{(r)}\right)^{-1}. \tag{4}$$

Because of isotropy, the effective stiffness at Level I is fully specified by the effective bulk, $K_{\mathrm{eff}}^{\mathrm{I}}$, and shear, $G_{\mathrm{eff}}^{\mathrm{I}}$, moduli

$$K_{\mathrm{eff}}^{\mathrm{I}} = \frac{c^{(0)}K^{(0)} + \sum_{r=1}^{m} c^{(r)}K^{(r)}A_{\mathrm{dil,V}}^{(r)}}{c^{(0)} + \sum_{r=1}^{m} c^{(r)}A_{\mathrm{dil,V}}^{(r)}},$$